Polymer Journal (2024) 56:193–204
https://doi.org/10.1038/s41428-023-00865-7

ORIGINAL ARTICLE

Design of dual stimuli-responsive gels with physical and chemical properties that vary in response to light and temperature and cell behavior on their surfaces

Masaaki Okihara[1] · Akana Matsuda[1] · Akifumi Kawamura[1,2] · Takashi Miyata[1,2]

Received: 16 October 2023 / Revised: 14 November 2023 / Accepted: 16 November 2023 / Published online: 26 December 2023

Abstract

Cell behaviors are highly sensitive to the surrounding environment. Therefore, in regulating cells, biomaterial substrates should be designed so their properties are similar to the surrounding environments of the cells. For cell regulation, we designed dual stimuli-responsive gels whose physical (elastic modulus) and chemical (hydrophilicity) properties can be changed by varying the UV exposure time and temperature, respectively. A dual stimuli-responsive polymer with photodimerizable groups and temperature-responsive moieties was prepared by copolymerizing 7-methacryloyloxycoumarin (MAC) and methoxyoligoethylene glycol methacrylate (OEGMA). The resulting polymers (P(MAC-*co*-OEGMA)) had lower critical solution temperatures (LCSTs), which depended on the compositions. A buffer solution containing P(MAC-*co*-OEGMA) was exposed to ultraviolet light (UV) for gelation, and the elastic modulus increased with increasing exposure time. The cell behavior, including adhesion and spreading, on the surfaces of these gels was investigated. Most of the cells adhered to P(MAC-*co*-OEGMA) gels with higher elastic moduli, and the cells were spread more effectively at temperatures above the LCST. This was because cell adhesion and spreading were strongly influenced by the physical and chemical properties of the P(MAC-*co*-OEGMA) gels, which were regulated by varying the UV exposure time and temperature.

Introduction

Cells exist in cellular environments comprising polysaccharides, proteins, and proteoglycans. The biochemical, physicochemical, and structural-dynamic factors of the extracellular matrix (ECM) vary spatiotemporally [1]. Cells recognize the above factors in their environment and change their behavior accordingly [2, 3]. Biochemical factors [4], such as hormones and cytokines, and physicochemical factors [5], such as pH and temperature, play important roles in determining the cellular environment. In mechanobiology, cell adhesion, spreading, migration, proliferation, and differentiation are influenced by structural and mechanical factors, such as the shapes and elastic moduli of the scaffolds [6–13]. Engler et al. reported that when cultured on gel substrates with distinct elastic moduli, stem cells [14] and cardiomyocytes [15] perceived the elastic modulus and changed their differentiation and extension behaviors accordingly. Since then, many studies on mechanobiology have focused on the physical forces and changes contributing to cell behaviors, such as proliferation, spreading, and differentiation. Additionally, many scientists have tried to manipulate cell behavior by tuning the physical properties of the scaffolds, such as the stiffness and viscoelasticity. Although many studies were designed to control cell behaviors with scaffolds with different elastic moduli, most of the scaffolds exhibited static physical properties. Moreover, as cells are constantly exposed to dynamic environmental changes in vivo, spatiotemporal control of the physical and chemical properties of scaffolds is necessary to clarify the environmental effects on cell behavior and to regulate cell fates.

Supplementary information The online version contains supplementary material available at https://doi.org/10.1038/s41428-023-00865-7.

✉ Takashi Miyata
tmiyata@kansai-u.ac.jp

[1] Department of Chemistry and Materials Engineering, Kansai University, 3-3-35, Yamate-cho, Suita, Osaka 564-8680, Japan

[2] Organization for Research and Development of Innovative Science and Technology, Kansai University, 3-3-35, Yamate-cho, Suita, Osaka 564-8680, Japan

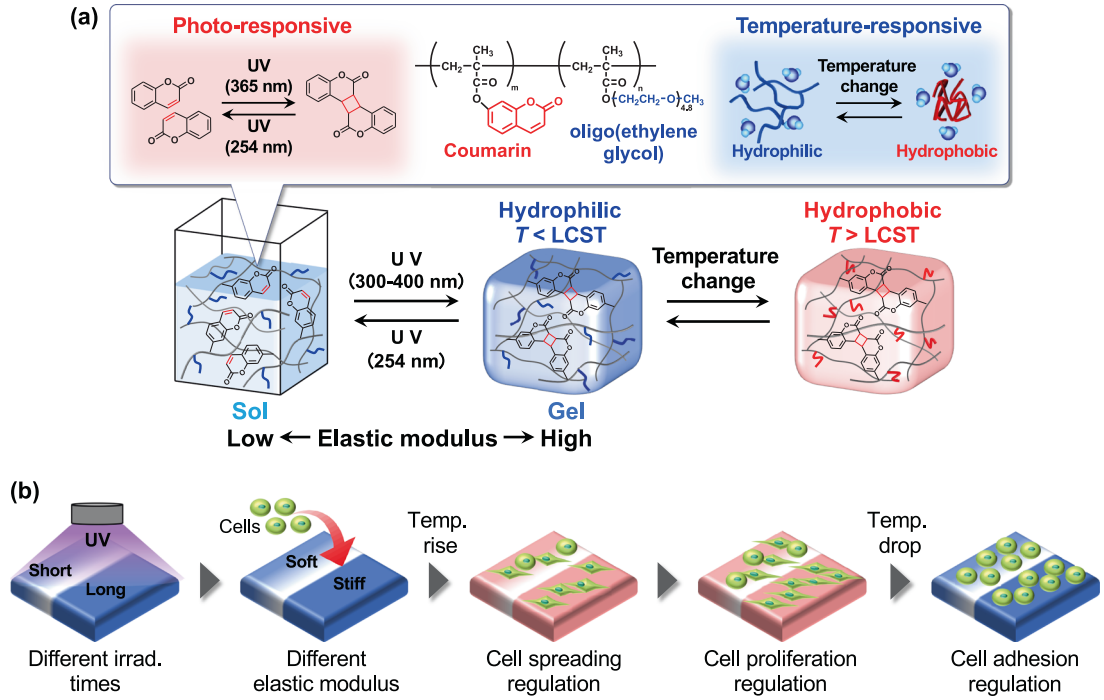

Fig. 1 **a** Strategic design of dual stimuli-responsive polymer gels exhibiting dynamic changes in their physical and chemical properties in response to variations in UV exposure time and temperature. **b** Schematic for cell regulation by tuning the elastic moduli and hydrophobicities/hydrophilicities of dual stimuli-responsive polymer gels

Hydrogels composed of three-dimensional polymer networks and abundant water exhibit unique properties, such as elasticity and hydrophilicity, similar to biological tissues. They have many potential applications in drug delivery, diagnostics, and cell cultures [16, 17]. Among hydrogels, some exhibit spontaneous changes in their structures and properties in response to external stimuli, such as temperature, pH, and light, and are called stimuli-responsive hydrogels. Because stimuli-responsive hydrogels can sense environmental changes as external stimuli and subsequently modify their intrinsic structures and properties [18–20], they have been widely used as intelligent materials for designing self-regulated drug delivery systems, sensors, and cell scaffolds [21–29]. For example, Okano et al. fabricated cell sheets by culturing cells on a temperature-responsive poly(*N*-isopropylacrylamide) (PNIPAAm) surface, which became hydrophobic with increasing temperature around its lower critical solution temperature (LCST) [30–32]. Furthermore, multistimuli-responsive polymers with photoreactive groups have also been studied intensively [33–38]. For example, photocrosslinked and photodegradable hydrogels that can change their mechanical properties, such as stiffness, in response to light exposure have been used as stimuli-responsive scaffolds to control cell behavior [39–45]. However, there have been few reports on multistimuli-responsive hydrogels that control their physical properties, such as elastic moduli, and their chemical properties, such as hydrophilicity/hydrophobicity, with light exposure time and temperature changes, respectively. Thus, most studies on mechanobiology have used hydrogels that exhibited changes in their chemical or physical properties in response to only one stimulus. To the best of our knowledge, there has been no report on cell culture on such multistimuli-responsive hydrogels with both changeable elastic moduli and hydrophilicities in response to multiple stimuli. Designing multistimuli-responsive hydrogels that can drastically change their chemical and physical properties in response to multiple stimuli, such as light and temperature, and regulate cell behavior using spatiotemporal changes in their properties is challenging.

Although most scientists have focused on temperature- and pH-responsive hydrogels, we previously designed molecularly stimuli-responsive hydrogels that changed their volumes in response to specific biomolecules, such as an antigen and a tumor marker [46–48]. These were designed using molecular complexes as dynamic crosslinks in their networks. Recently, we have also focused on photodimerizable groups as dynamic crosslinks for photoresponsive materials. For example, photoresponsive tetra-PEGs undergoing sol–gel phase transitions upon exposure to light were prepared by introducing photodimerizable groups to their chain ends [49]. In addition, we designed photocrosslinkable polymer films, whose surfaces formed micropatterns upon

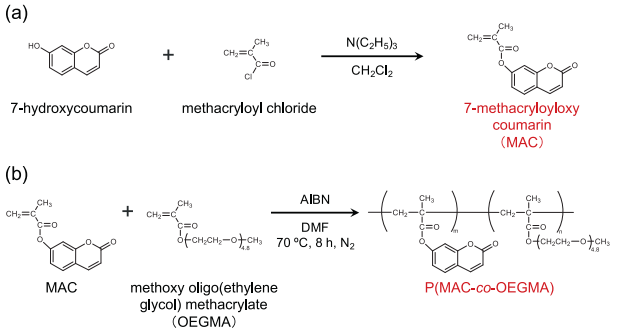

Scheme 1 Syntheses of (**a**) 7-methacryloyloxycoumarin (MAC) and (**b**) P(MAC-*co*-OEGMA)

irradiation with a photomask, and observed the formation of cell patterns on the micropatterned films [50, 51]. Therefore, hydrogels that change their properties in response to external stimuli are promising scaffolds for cell regulation, as they realize dynamic control of their surrounding environment. While dynamic crosslinks provide control of physical properties such as the elastic moduli of hydrogels, temperature-responsive polymer chains enable us to change their hydrophilicities/hydrophobicities. Thus, dual stimuli-responsive hydrogels that change their physical and chemical properties in response to two different stimuli can be synthesized by introducing dynamic crosslinks into the temperature-responsive polymer chains.

In this paper, we report dual stimuli-responsive polymers that drastically changed their physical and chemical properties in response to light and temperature for spatiotemporal control of cellular behavior. These polymers were synthesized by copolymerization of 7-methacryloyloxycoumarin (MAC) [52–54], which exhibited reversible photodimerization, and methoxyoligoethylene glycol methacrylate (OEGMA) [55], with an LCST. An aqueous solution of the resulting polymer (P(MAC-*co*-OEGMA)) underwent distinct gelation upon UV exposure because light-induced coumarin photodimerization resulted in the formation of crosslinks in the polymer chains. Furthermore, we investigated the effects of the UV exposure time and temperature on the elastic moduli and hydrophilicities/hydrophobicities of the resulting P(MAC-*co*-OEGMA) hydrogels (Fig. 1a). Additionally, cell behavior on hydrogel surfaces with varying elastic moduli and hydrophilicities/hydrophobicities were examined as a function of the UV exposure time and temperature (Fig. 1b). Unlike previous studies on cell behavior, where stimuli-responsive hydrogels exhibited changes in their physical or chemical properties in response to only one stimulus, this paper focuses on the physical and chemical properties of dual stimuli-responsive hydrogels, which can be tuned by varying the UV exposure time and temperature, to realize spatiotemporal control of cells. Dual stimuli-responsive hydrogels with changeable elastic moduli and hydrophilicity/hydrophobicity have many potential applications because they are novel biomaterials that enable spatiotemporal control of cell behavior, unlike standard studies in the field of mechanobiology focusing on only mechanical factors.

Experimental procedures

Materials

7-Hydroxycoumarin was purchased from Tokyo Chemical Industry Co., Ltd (Tokyo, Japan). Chloroform, methanol, tetrahydrofuran (THF), *N,N*-dimethylformamide (DMF), dichloromethane (DCM), 2,2′-azobis(isobutyronitrile) (AIBN), deuterated chloroform ($CDCl_3$-*d*), and tetramethylsilane (TMS) were procured from Fujifilm Wako Pure Chemical Co. (Osaka, Japan). Oligo(ethylene glycol) methyl ether methacrylate (OEGMA, $M_n = 300$) was purchased from Sigma–Aldrich (St. Louis, USA). The mouse fibroblast line (L929) used in cell culture experiments was purchased from RIKEN BioResource Center (Ibaraki, Japan). Eagle's minimal essential medium (E-MEM), glutamine, and Dulbecco's phosphate-buffered saline (−) (D-PBS(−)) were purchased from Shimadzu Diagnostics Co. (Tokyo, Japan). Funakoshi Co., Ltd. (Tokyo, Japan) supplied fetal bovine serum (FBS). Calcein-AM dye was purchased from Dojindo Laboratories (Kumamoto, Japan). Other solvents and reagents of analytical grade were obtained from commercial sources and used without further purification.

Synthesis of MAC

Scheme 1(a) presents the synthetic strategy for preparing 7-methacryloyloxycoumarin (MAC). 7-Hydroxycoumarin (6.45 g, 0.04 mol) and TEA (8.18 g, 0.08 mol) were dissolved in dehydrated DCM (100 mL). Methacryloyl chloride (5.09 g, 0.05 mol) was then separately dissolved in dehydrated DCM (100 mL) and added dropwise to the 7-hydroxycoumarin solution over 30 min in an ice bath. The resulting mixture was then stirred at room temperature overnight. After completion of the reaction, the excess solvent was removed under reduced pressure; furthermore, the desired product was dissolved in 160 mL of chloroform, washed thrice with 160 mL of Milli-Q water (MQ), and collected in an organic layer. The organic layer was dried over anhydrous magnesium sulfate and filtered, and the solvent was removed with a rotary evaporator to give a light orange solid. The light orange solid obtained was dissolved in a mixture of methanol and THF in a 2:1 (v/v) ratio, amounting to 90 mL, and warmed at 50 °C. After leaving this solution undisturbed overnight at 25 °C, the substance

was recrystallized and filtered with suction, yielding MAC (yield: 65%). Successful synthesis of MAC was confirmed via proton nuclear magnetic resonance (^{1}H NMR, Fig. S1). ^{1}H NMR spectra were recorded on a JNM-AL400 spectrometer (JEOL Co., Ltd, Tokyo, Japan) operating at 400 MHz with $CDCl_3$-*d* as the solvent and TMS as the internal standard.

Syntheses of polymers

Poly(7-methacryloyloxycoumarin-*co*-oligo(ethylene glycol) methyl ether methacrylate) (P(MAC-*co*-OEGMA)) and poly(oligo(ethylene glycol) methyl ether methacrylate) (POEGMA) were synthesized via free radical polymerization (Scheme 1(b)). Table S1 summarizes the feed compositions for the syntheses of P(MAC-*co*-OEGMA) and POEGMA. OEGMA ($M_w = 295$) was purified on an alumina column and dissolved in DMF along with MAC ($M_w = 230.2$). To this solution, 2.0 mol% of AIBN, recrystallized from methanol, was added. Furthermore, freeze–pump–thaw cycles were used to remove the residual oxygen, and subsequently, copolymerization was carried out at 70 °C for 8 h under a nitrogen atmosphere. The resulting polymer solution was introduced into a cellulose dialysis membrane with a molecular weight cutoff of 3.5 kDa and dialyzed against methanol (500 mL) for a period of 3 days to remove any residual monomer and initiator. The dialysate was replaced five times throughout this process. Finally, the solvent was removed under reduced pressure, yielding a clear, viscous liquid. Successful synthesis of the polymer was confirmed by the ^{1}H NMR spectra (Figs. S2–S4).

Photodimerization of P(MAC-*co*-OEGMA)

P(MAC-*co*-OEGMA) was dissolved in chloroform at a concentration of 0.2 mg/mL. Next, the resulting solutions were exposed to UV light within the 300–400 nm range (20 mW/cm^2) from a xenon light source (MAX-303: Asahi Spectra Co., Ltd, Tokyo, Japan) for various times with a heat absorption filter. A UV–Vis spectrophotometer (UV-2550: Shimadzu Co., Kyoto, Japan) was used to measure their UV–Vis spectra. Additionally, to measure the dissociation behavior, the polymer solution was irradiated with a xenon light source (MAX-303: Asahi Spectra Co., Ltd, Tokyo, Japan) and a 254 nm bandpass filter (0.05 mW/cm^2).

Rheological measurements of P(MAC-*co*-OEGMA)

The rheological measurements were performed under a constant strain of 1% and frequency range of 0.015–15.9 Hz at 25 °C using a RheoStress 300 (Anton Paar, Japan, MCR102). The storage moduli (G') and loss moduli (G'') of the solutions or hydrogels were evaluated at a frequency of 1 Hz under constant strain.

Transmittance measurements

The temperature responses of PBS(−) solutions of P(MAC-*co*-OEGMA) and POEGMA were evaluated by measuring their transmittances as a function of temperature at 650 nm with a UV–visible spectrometer (UV-2550: Shimadzu, Kyoto, Japan). Hydrogels were prepared by placing P(MAC-*co*-OEGMA) solutions in quartz glass molds and irradiating them with UV light (300–400 nm).

Cell culture on P(MAC-*co*-OEGMA) gels

After P(MAC-*co*-OEGMA) was dissolved in PBS(−) at a concentration of 28 wt%, the resulting pregel solution was cast on a tissue culture polystyrene (TCPS) dish. Subsequently, gels were formed by exposing the pregel solution to UV light from a xenon light source (MAX-303) equipped with a heat-absorbing filter (300–400 nm) for a predetermined duration. The resulting gels were washed three times with PBS(−) and subsequently incubated with 10% FBS/EMEM (1 mL) at 37 °C and 5% CO_2 overnight. Afterward, L929 cells suspended in 10% FBS/EMEM were seeded onto the prepared gels at predetermined cell densities and maintained in EMEM supplemented with 10% FBS at 37 °C under a humid atmosphere containing 5% CO_2.

Once the gels were prepared by irradiating the pregel solutions with the xenon light source (MAX-303) with a heat-absorbing filter (300–400 nm) for 1 h, micropatterns were fabricated by exposing these gels to UV light through a grid-shaped photomask (pitch = 250 mm, hole = 200 mm, and bar = 50 mm) for 1 h. L929 cells suspended in 10% FBS/EMEM were seeded onto these micropatterned gels at predetermined cell densities and placed in EMEM supplemented with 10% FBS at 37 °C under a humid atmosphere with 5% CO_2.

The behaviors of the L929 cells at various culture temperatures were evaluated by changing the culture temperature after cell adhesion. L929 cells suspended in 10% FBS/EMEM were seeded onto a TCPS dish and P(MAC-*co*-OEGMA) gels at predetermined cell densities and placed in EMEM supplemented with 10% FBS at 30 °C or 37 °C under a humid atmosphere with 5% CO_2. Furthermore, the effect of culture temperature on cell behavior was investigated by reducing the culture temperature from 37 °C to 30 °C at random times. The behavior of the L929 cells on P(MAC-*co*-OEGMA) gels and TCPS dishes was monitored with a fluorescence microscope (BZ-X710: KEYENCE Co., Osaka, Japan).

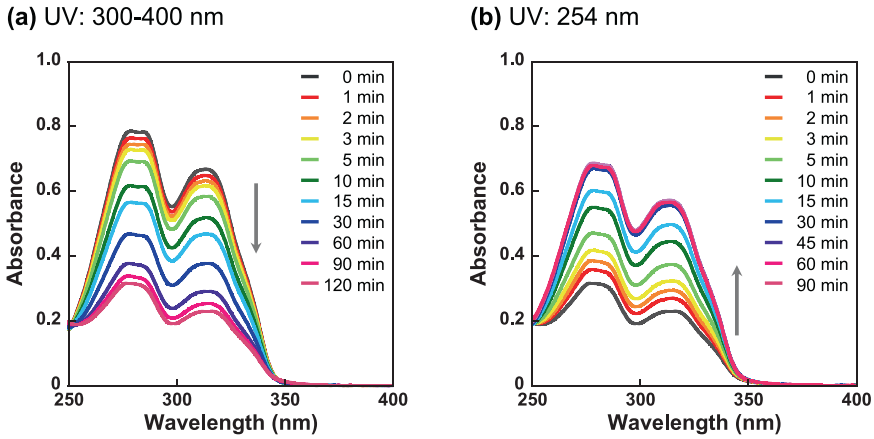

Fig. 2 UV–Vis spectra of P(MAC-*co*-OEGMA) with a MAC content of 20 mol% in chloroform after exposure to UV wavelengths of **a** 300–400 and **b** 254 nm for various durations. The concentration of P(MAC-*co*-OEGMA) in the chloroform solution was 0.2 mg/mL

Results and discussion

Synthesis of P(MAC-*co*-OEGMA)

MAC bearing a photodimerizable coumarin group was synthesized according to Scheme 1a. The ^{1}H NMR spectrum of MAC exhibited characteristic peaks at 6.0 and 6.3 ppm, which were attributed to the protons of the CH_2=C double bond, implying successful incorporation of the double bond into coumarin (Fig. S1). The resulting MAC was copolymerized with OEGMA to synthesize P(MAC-*co*-OEGMA) (Scheme 1b). The ^{1}H NMR spectrum of P(MAC-*co*-OEGMA) revealed the disappearance of peaks for the double bonds of MAC and OEGMA (Figs. S2–S4). Furthermore, the peaks derived from P(MAC-*co*-OEGMA) broadened, and their integrated values matched the theoretical values, confirming successful synthesis of P(MAC-*co*-OEGMA) as an amphiphilic polymer with photodimerizable groups. The molar ratio of MAC to OEGMA in P(MAC-*co*-OEGMA) was determined from the peaks at 6.4 ppm for MAC and 4.2 ppm for OEGMA, yielding MAC:OEGMA = 20.2:79.8 (mol%).

Photodimerization of P(MAC-*co*-OEGMA)

Reversible photodimerization of P(MAC-*co*-OEGMA) was analyzed with UV–Vis spectroscopy. Figure 2a shows the UV–Vis spectrum of P(MAC-*co*-OEGMA) in chloroform irradiated with UV at wavelengths of 300–400 nm for various durations. The absorbances of the coumarin groups at 280 and 330 nm decreased with increasing UV exposure time. After excitation of the coumarin groups by UV exposure, they underwent photo[2 + 2] cyclizations with the neighboring coumarin groups, followed by the formation of cyclobutane rings and generation of coumarin dimers [56, 57]. This indicated that P(MAC-*co*-OEGMA) underwent photodimerization upon exposure to UV light with wavelengths of 300–400 nm. Subsequently, a solution of P(MAC-*co*-OEGMA) in chloroform was exposed to UV light with a wavelength of 254 nm for various durations. Figure 2b shows that the UV–Vis spectra of the photodimerized P(MAC-*co*-OEGMA) changed further with continuous exposure to 254 nm UV light, and the absorbance of the coumarin groups increased with increasing exposure time. This increased absorbance was attributed to photocleavage of the cyclobutane rings within the coumarin dimer upon exposure to high-energy 254 nm UV light, which led to the formation of coumarin monomers. The slow recovery of coumarin monomer absorbance might indicate that symmetrically and asymmetrically cleaved coumarin derivatives were produced via cyclobutane ring photocleavage [58]. Changes in the UV–Vis spectrum of P(MAC-*co*-OEGMA) upon UV exposure revealed that the coumarin groups in P(MAC-*co*-OEGMA) formed dimers upon UV exposure at 300–400 nm, and photocleavage of the coumarin dimers induced by UV exposure at 254 nm produced coumarin monomers. This implied that the UV wavelength determined reversible photodimerization of P(MAC-*co*-OEGMA).

Viscoelasticities of P(MAC-*co*-OEGMA) gels

The previous section revealed that the coumarin groups of P(MAC-*co*-OEGMA) underwent reversible photodimerization during UV exposure. This means that P(MAC-*co*-OEGMA) can be crosslinked to form gels upon exposure to UV light. We investigated gelation of PBS(-) with P(MAC-*co*-OEGMA) with an MAC content of 20 mol% by exposing the mixture to UV with wavelengths of 300–400 nm and determined the physical properties of the resulting gels as a function of the exposure time. An aqueous P(MAC-*co*-OEGMA) solution underwent a phase transition from a sol state to a gel state when exposed to UV light with wavelengths of 300–400 nm (Fig. 3a). The viscoelasticity of an aqueous P(MAC-*co*-OEGMA) solution was also investigated with a rheometer after UV exposure. Figure 3b demonstrates

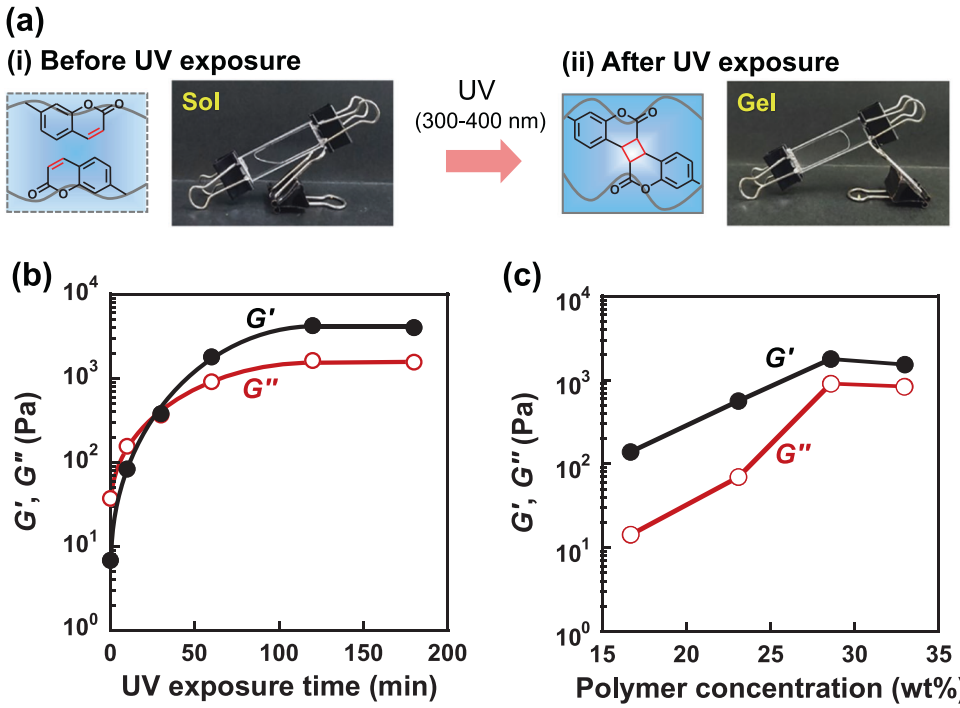

Fig. 3 **a** Photographs of water containing P(MAC-*co*-OEGMA) with 20 mol% MAC (i) before and (ii) after exposure to UV wavelengths of 300–400 nm for 1 h. The concentration of P(MAC-*co*-OEGMA) with 20 mol% MAC was 33 wt% in water. **b** Effect of the UV (300–400 nm) exposure time on the storage modulus (*G'*, closed circle) and loss modulus (*G″*, open circle) of the P(MAC-*co*-OEGMA) gel with 20 mol% MAC. Aqueous P(MAC-*co*-OEGMA) solutions were exposed to UV for 1 h before the rheological measurements. **c** Effect of the polymer concentration on the storage modulus (*G′*, closed circle) and loss modulus (*G″*, open circle) of the P(MAC-*co*-OEGMA) gel with 20 mol% MAC. The polymer concentration of P(MAC-*co*-OEGMA) with 20 mol% MAC was 28 wt% in PBS(−).

the effect of the UV exposure time on the storage modulus (*G′*) and loss modulus (*G″*) of an aqueous P(MAC-*co*-OEGMA) solution with a polymer concentration of 28 wt% after exposure to UV at wavelengths of 300–400 nm. *G′* and *G″* increased gradually with increasing UV exposure times. Importantly, while *G′* of the aqueous P(MAC-*co*-OEGMA) solution was lower than *G*" when the UV exposure time was <30 min, the former became greater than the latter upon increasing the UV exposure time further. In addition, the frequency dependence of *G′* and *G″* indicated that *G′* of the aqueous P(MAC-*co*-OEGMA) solution after UV exposure for more than 30 min was greater than *G″* for a wide range of frequencies, unlike that seen after UV exposure for less than 30 min (Fig. S5). This means that UV exposure for more than 30 min induced gelation of the aqueous P(MAC-*co*-OEGMA) solution with a polymer concentration of 28 wt%. The photoresponsive gelation of the aqueous P(MAC-*co*-OEGMA) solution was attributed to formation of a crosslinked network via coumarin photodimerization. Notably, the increases in *G*' for the resulting P(MAC-*co*-OEGMA) gel with prolonged UV exposure indicated that the stiffness could be regulated by adjusting the UV exposure time. Furthermore, the *G′* and *G″* values for an aqueous P(MAC-*co*-OEGMA) solution after UV exposure strongly depended on the polymer concentration (Fig. 3c). When aqueous P(MAC-*co*-OEGMA) solutions with various polymer concentrations were exposed to UV wavelengths of 300–400 nm for 1 h, their *G′* and *G″* values increased gradually with increasing polymer concentration. The frequency dependence of *G′* and *G″* demonstrated that the *G′* value of the aqueous P(MAC-*co*-OEGMA) solutions after UV exposure for 1 h was greater than *G″* over a wide range of frequencies (Fig. S6). An aqueous P(MAC-*co*-OEGMA) solution with a higher polymer concentration formed a crosslinked network more easily than that with a lower polymer concentration. Thus, the resulting P(MAC-*co*-OEGMA) gel had phototunable physical properties such as an elastic modulus that was regulated by the UV exposure time.

Temperature response of P(MAC-*co*-OEGMA)

The LCSTs of temperature-responsive polymers such as PNIPAAm are the temperatures at which their solubilities in water change dramatically. For example, PNIPAAm is soluble in water at temperatures lower than 32 °C but becomes insoluble at temperatures higher than 32 °C. Such temperature-responsive changes in solubility are induced by drastic changes in the nature of the polymer chains from

hydrophilic to hydrophobic with increasing temperature. Similar to PNIPAAm, POEGMA produced via polymerization of OEGMA had an LCST of 65 °C [55]. We investigated the temperature-responsive behavior of P(MAC-*co*-OEGMA) or POEGMA in PBS(−) by measuring its transmittance at 650 nm at various temperatures (Fig. 4a). The transmittance (100%) of an aqueous POEGMA solution remained constant with increasing temperature up to 60 °C, indicating that POEGMA is soluble in PBS(−) over the temperature range 25–60 °C. Meanwhile, the transmittance of PBS(−) containing P(MAC-*co*-OEGMA) with MAC contents of 16 and 20 mol % decreased dramatically from 100% to 0% at 37 °C and 33 °C, respectively. Notably, PBS(−) with P(MAC-*co*-OEGMA) exhibited a sharp decline in transmittance near body temperature. The LCST of POEGMA, the homopolymer of OEGMA used in this study, is approximately 65 °C [55]. These findings underscore the presence of LCSTs for the synthesized polymers beyond which they become insoluble in water. This is because the interactions between the polymer chains and water molecules are stable below the LCST, so the polymers are soluble in water [59]. However, above the LCST, this balanced interaction is disrupted in favor of hydrophobic interactions, causing dehydration and reduced polymer solubility in water [60]. Furthermore, the LCST can be regulated to a temperature close to body temperature by varying the hydrophobic MAC content. In OEGMA, the ether oxygens within the OEG moieties are the hydrophilic components, as they form stable hydrogen bonds with water molecules, while the main chains, comprising nonpolar carbon–carbon backbones, are the competitive hydrophobic component. Introduction of the hydrophobic MAC caused a shift in the LCST to a lower temperature because the P(MAC-*co*-OEGMA) became more hydrophobic than POEGMA [61, 62]. Therefore, the LCST of P(MAC-*co*-OEGMA) with a MAC content of 20 mol% was lower than that with 16 mol % MAC. This indicated that the LCST of P(MAC-*co*-OEGMA) could be tuned by varying the MAC content. In this study, P(MAC-*co*-OEGMA) with a MAC content of 20 mol% was used as a photo/temperature-responsive polymer because it became hydrophobic at 37 °C, at which point cells could be cultured on the gel surface.

Figure 4b shows the effect of temperature on the transmittance of the P(MAC-*co*-OEGMA) gel with an MAC content of 20 mol%, which was prepared by exposing an aqueous solution to UV wavelengths of 300–400 nm for 1 h. As the temperature was increased, the gel transmittance exhibited a steep decline at 33 °C, similar to that of an aqueous P(MAC-*co*-OEGMA) solution. Movie S1 demonstrates the rapid changes occurring in the P(MAC-*co*-OEGMA) gel from transparent to turbid when it was immersed in water at 40 °C. These results indicated that the P(MAC-*co*-OEGMA) gel maintained its temperature responsiveness, even though the polymer chains were photocrosslinked via photodimerization of the coumarin groups. Furthermore, to evaluate the changes in hydrophilicity/hydrophobicity in response to temperature, we measured the contact angle of an air bubble on the P(MAC-*co*-OEGMA) gel in water (Fig. 4c). The contact angles on the P(MAC-*co*-OEGMA) gel were 142.3° at 25 °C (lower than the LCST) and 133.5° at 55 °C (higher than the LCST). Generally, the contact angle of an air bubble on a hydrophilic surface in water is higher than that on a hydrophobic surface. Therefore, the contact angle measurements revealed that the P(MAC-*co*-OEGMA) gel was hydrophilic below the LCST of the polymer chain and became less hydrophilic above the LCST. These results were consistent with the temperature-dependent transmittances exhibited by the P(MAC-*co*-OEGMA) gel. However, even though the P(MAC-*co*-OEGMA) chain became insoluble in water above its LCST, the surface of the P(MAC-*co*-OEGMA) gel was not very hydrophobic, unlike those of other temperature-responsive polymers such as PNIPAAm. Thus, the P(MAC-*co*-OEGMA) gel was swollen and transparent in water owing to the hydrophilicity of its polymer chains below the LCST. An increase in temperature above the LCST induced dehydration and aggregation of the polymer chains, which reduced the hydrophilicities of the gels. Therefore, the chemical properties, such as hydrophilicity/hydrophobicity, of the P(MAC-*co*-OEGMA) gel were altered by small changes in temperature because it had an LCST of 33 °C, implying that the gel is a promising scaffold for cell regulation.

Cell behavior on P(MAC-*co*-OEGMA) gels with different elastic moduli

Physical properties such as the elastic moduli of gels are important in governing cell behavior such as adhesion, spreading, and proliferation. We investigated the cell behavior on P(MAC-*co*-OEGMA) gels with different elastic moduli, which were formed by UV irradiation of aqueous P(MAC-*co*-OEGMA) solutions for different durations. The P(MAC-*co*-OEGMA) gels prepared by UV exposure for 30 and 60 min had elastic moduli of 0.4 and 1.6 kPa, respectively (Fig. 3b). Figure 5a shows phase contrast and fluorescence microscopy images of L929 cells cultured for 3 days on P(MAC-*co*-OEGMA) gels prepared by UV exposure for 30 and 60 min. The images demonstrate that more cells were adhered on the gel with an elastic modulus of 1.6 kPa than on the gel with an elastic modulus of 0.4 kPa. Interestingly, the cells on gels with higher elastic moduli spread more efficiently than those on gels with lower elastic moduli. Additionally, the fluorescence microscopy images exhibited green emission in the regions where cells were adhered. This indicated that the cells proliferated on the

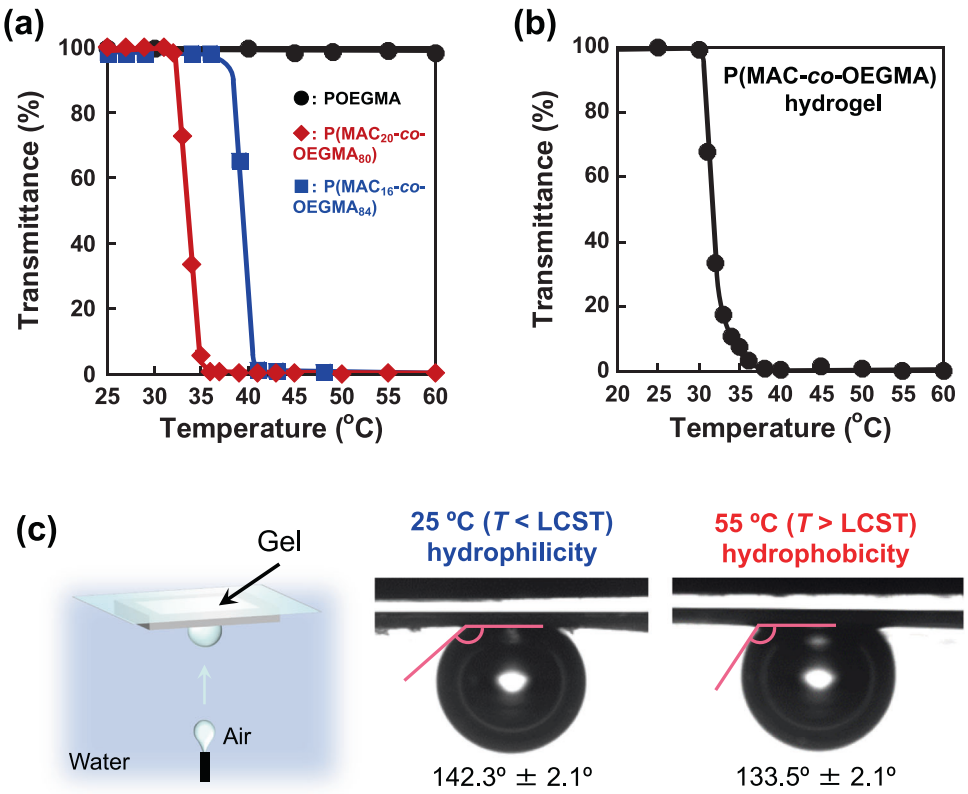

Fig. 4 **a** Effect of temperature on the transmittance (at 650 nm) of PBS(−) containing POEGMA (●) and P(MAC-*co*-OEGMA) with MAC concentrations of 16 (■) and 20 mol% (◆). The polymer concentration was 5.0 mg/mL. **b** Effect of temperature on the transmittance (wavelength, 650 nm) of the P(MAC-*co*-OEGMA) gel with 20 mol% MAC prepared via UV (300–400 nm) exposure for 1 h. **c** Contact angles of an air bubble on the P(MAC-*co*-OEGMA) hydrogel with 20 mol% MAC in water at 25 °C and 37 °C. The gel was prepared by UV (300–400 nm) exposure for 2 h

P(MAC-*co*-OEGMA) gel and maintained their vitality without cytotoxic effects. Importantly, the cells were cultured on the P(MAC-*co*-OEGMA) gel at 37 °C, which was higher than the LCST of the P(MAC-*co*-OEGMA) chain. As the P(MAC-*co*-OEGMA) gel had a hydrophobic surface at 37 °C, cells adhered easily. Moreover, Fig. 5b demonstrates that the density of cells on the gel with an elastic modulus of 0.4 kPa was $9.3 \times 10^5/cm^2$, whereas that on a gel with an elastic modulus of 1.6 kPa was $15.1 \times 10^5/cm^2$. Some tissues have high elastic moduli, and others have low elastic moduli in vivo [63]. Therefore, cells should be cultured in a suitable environment with a specific elastic modulus [15, 64]. The L929 cells used in this study were of the fibroblast lineage. As fibroblasts typically have elastic moduli in the range of 2–3 kPa, L929 cells might adhere, spread, and proliferate on the P(MAC-*co*-OEGMA) gel with an elastic modulus of 1.6 kPa more readily than on the gel with an elastic modulus of 0.4 kPa. These results implies that cell behaviors, such as adhesion, spreading, and proliferation, were regulated with the phototunable elastic modulus of the P(MAC-*co*-OEGMA) gel.

After the P(MAC-*co*-OEGMA) gel with a phototunable elastic modulus was prepared by exposing the aqueous solution of P(MAC-*co*-OEGMA) with an MAC content of 20 mol% to UV, a micropattern with regions of high and low elastic moduli was formed on the gel after UV exposure for 120 min through a photomask (Fig. S7). Figure 5c and Movie S2 show phase contrast microscopy images and time-lapse videos of the L929 cells, respectively, while they were cultured on gels with a micropatterned surface for 48 h. The cells congregated, adhered, and spread in regions with high elastic moduli more preferentially than in those with low elastic moduli. Furthermore, the cells that adhered to the regions with high elastic moduli proliferated considerably after 48 h. This result was supported by the fact that the numbers of cells adhering to and proliferating on the gel surface with a high elastic modulus were greater than those adhering and proliferating on the gel surface with a low elastic modulus (Fig. 5a). Hence, cell behaviors such as adhesion, spreading, and proliferation can be regulated by varying the elastic modulus of the P(MAC-*co*-OEGMA) gel, which in turn can be optimized by varying the UV exposure time.

Cell behavior on P(MAC-*co*-OEGMA) gels with different hydrophobicities/hydrophilicities

Cell behavior is influenced by physical properties such as the elastic moduli and chemical properties such as the hydrophobicities/hydrophilicities of the scaffolds. For example, cells adhere more readily to hydrophobic surfaces, but they are less likely to adhere to hydrophilic surfaces. Okano et al. developed a cell sheet technology in which cell sheets were prepared by enabling drastic changes in the

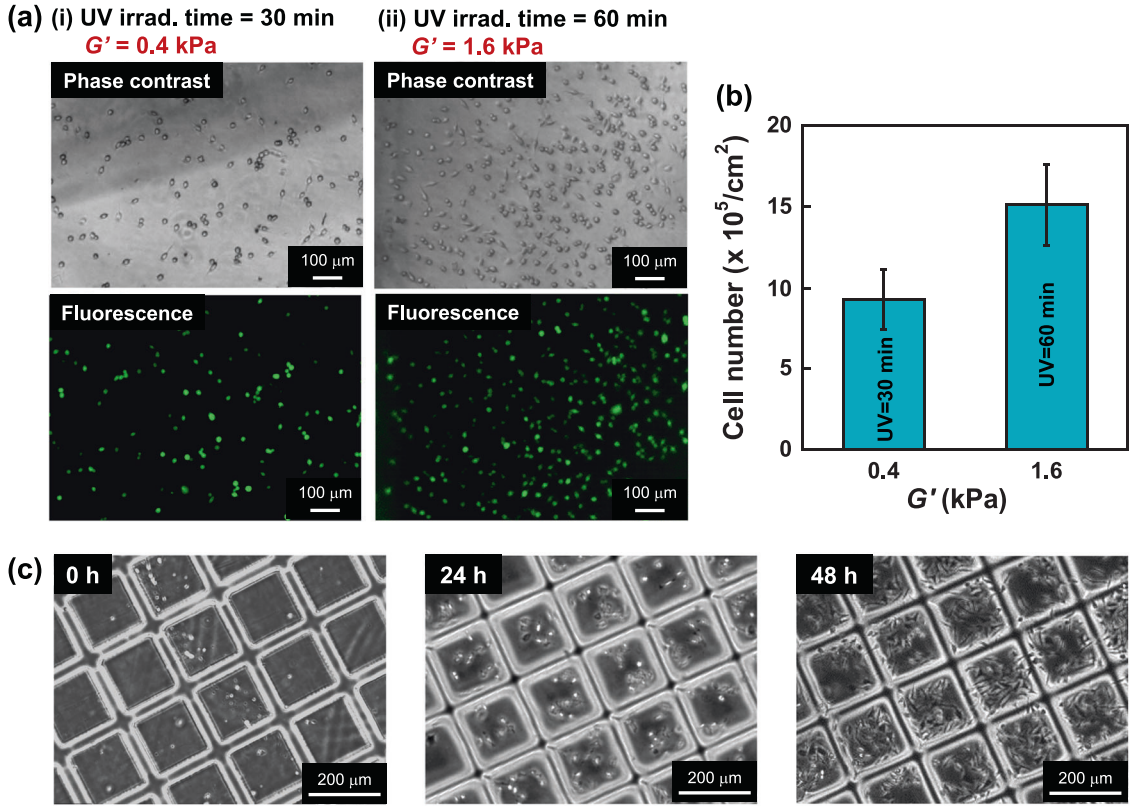

Fig. 5 **a** Phase contrast and fluorescence microscope images of L929 cells on the surface of P(MAC-*co*-OEGMA) gels with 20 mol% MAC. The gels were prepared by exposing PBS(−) containing P(MAC-*co*-OEGMA) to UV wavelengths of 300–400 nm for (i) 30 and (ii) 60 min. Cells were cultured on the gel surfaces for 3 days and stained with calcein. **b** Relationship between the storage modulus of P(MAC-*co*-OEGMA) gels with 20 mol% MAC and the number of cells that adhered on their surfaces for 3 days. **c** Optical microscopy images of L929 cells on a micropatterned surface of the P(MAC-*co*-OEGMA) gel with 20 mol% MAC after culturing the cells for 0, 24, and 48 h. The micropattern was prepared by exposing the P(MAC-*co*-OEGMA) gel to UV (300–400 nm) for 2 h through a photomask with a large square mesh shape (pitch = 250 μm, hole = 200 μm, and bar = 50 μm)

hydrophobicities/hydrophilicities of PNIPAAm substrates in response to temperature [27, 65]. This meant that the temperature-responsive hydrophilic/hydrophobic changes were useful tools for regulating cell behavior. In this study, we investigated cell behavior on the P(MAC-*co*-OEGMA) gel at temperatures lower and higher than the LCST of the P(MAC-*co*-OEGMA) chains.

Figure 6a shows the behavior of L929 cells on a P(MAC-*co*-OEGMA) gel with an MAC content of 20 mol% and TCPS as a reference at 30 °C and 37 °C. When cultured on the surfaces of the P(MAC-*co*-OEGMA) gel and TCPS, the number of L929 cells adhered at 37 °C was greater than that adhered at 30 °C. This was because the cells were more likely to proliferate at 37 °C than at 30 °C. Interestingly, while the L929 cells spread on the TCPS surface at 30 °C and 37 °C, they spread on the P(MAC-*co*-OEGMA) gel only at 37 °C. This occurred because the TCPS surface did not change its hydrophobicity in response to temperature changes; however, the P(MAC-*co*-OEGMA) gel had hydrophilic and hydrophobic surfaces at 30 and 37 °C, respectively. At 30 °C, the hydrophilic surface of the P(MAC-*co*-OEGMA) gel prevented cell adhesion because the adsorption of adhesion proteins such as fibronectins was inhibited by the exclusion volume effect of the oligo(ethylene glycol) chains. However, as the P(MAC-*co*-OEGMA) gel became hydrophobic at 37 °C, cells adhered and spread on its surface.

Additionally, we investigated the behavior of cells on the P(MAC-*co*-OEGMA) gel when the culture temperature was reduced to 25 °C for 1 h after culture at 37 °C for 1 day. The cells that spread on the P(MAC-*co*-OEGMA) gel at 37 °C transitioned into spherical shapes within 1 h after the culture temperature was switched from 37 °C to 25 °C (Fig. 6b, Movie S3). This indicated that cell detachments were induced by drastic changes in the gel surface from hydrophobic to hydrophilic in response to a change in temperature, similar to the studies reported by Okano et al. [27, 65]. Thus, the dynamic changes in the hydrophobicity/hydrophilicity of the P(MAC-*co*-OEGMA) gel in response to temperature were useful in regulating the cell behavior, such as adhesion and spreading. The phototunable physical properties and temperature-switchable chemical properties exhibited by the dual stimuli-responsive P(MAC-*co*-OEGMA) gel implied that

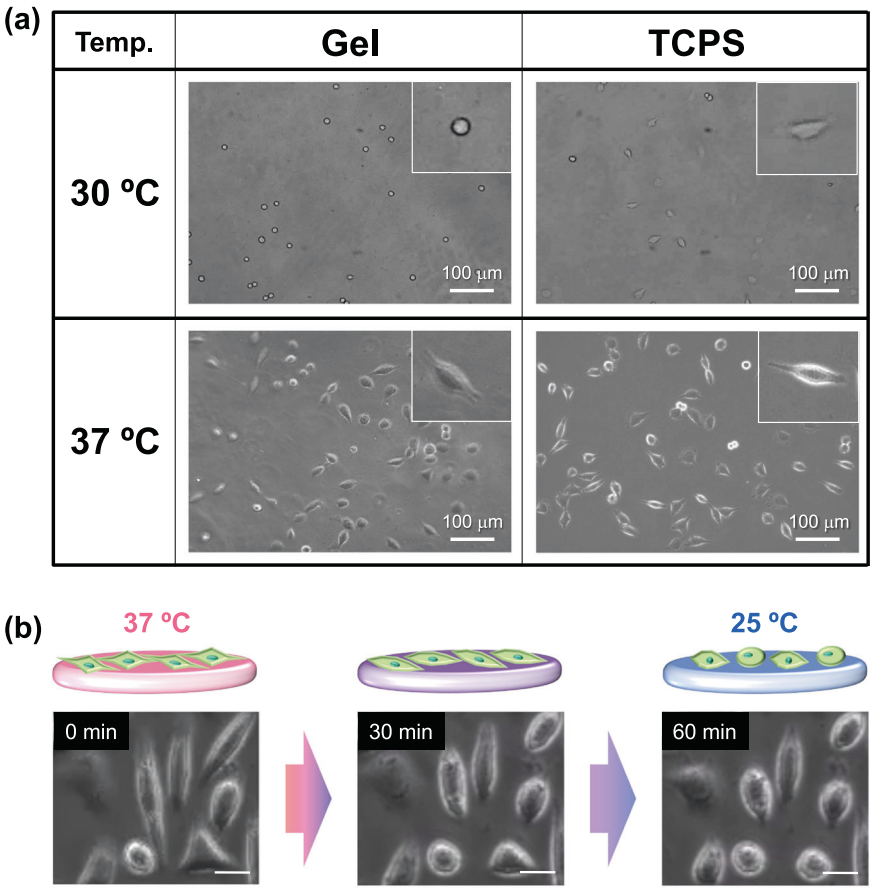

Fig. 6 **a** Phase contrast microscopy images of L929 cells on the surfaces of polystyrene dishes (TCPS) and P(MAC-*co*-OEGMA) gels with 20 mol% MAC formed by UV (300–400 nm) exposure for 180 min. Cells were cultured on their surfaces at 30 °C and 37 °C for 1 day. **b** Phase contrast microscopy images of L929 cells on the surfaces of P(MAC-*co*-OEGMA) gels with 20 mol% MAC when the temperature was switched from 37 °C to 25 °C. Scale bar: 20 μm

it has many future applications as a scaffold for regulating cell behavior.

Conclusion

We synthesized photo- and temperature-responsive P(MAC-*co*-OEGMA) as a dual stimuli-responsive polymer featuring photodimerizable coumarin groups and OEG with an LCST in its side chain. An aqueous P(MAC-*co*-OEGMA) solution underwent a phase transition from a sol to gel upon UV exposure. The elastic modulus of the resulting P(MAC-*co*-OEGMA) gel could be precisely regulated by varying the UV exposure time. Additionally, P(MAC-*co*-OEGMA) dissolved in aqueous solutions at temperatures lower than 33 °C became insoluble at temperatures higher than 33 °C. The P(MAC-*co*-OEGMA) gel changed its behavior from hydrophilic to hydrophobic with increasing temperature. Exposure of the P(MAC-*co*-OEGMA) gel to UV light through a photomask led to micropattern formation, comprising two regions with different elastic moduli. The cell cultured on the micropatterned surface demonstrated that more cells adhered and spread on the surface with a high elastic modulus. Moreover, while the cells retained their spherical shapes on the P(MAC-*co*-OEGMA) gels at temperatures lower than the LCST of the P(MAC-*co*-OEGMA) chains, they were more likely to spread at temperatures higher than the LCST. When the culture temperature was reduced to 25 °C after the cells were cultured on the P(MAC-*co*-OEGMA) gel at 37 °C, cells that adhered and spread on the gel surface were detached from its surface. Therefore, because the elastic modulus and hydrophobicity/hydrophilicity of the P(MAC-*co*-OEGMA) gel underwent drastic changes in response to the UV exposure time and temperature, respectively, it is a very promising scaffold for regulating cell behaviors such as adhesion, spreading, and proliferation. Furthermore, fundamental research on the cell behavior on dual stimuli-responsive polymer gels is required for a better understanding of the physical and chemical properties of the scaffolds and cell behaviors and could lead to breakthroughs in cell manipulation for regenerative medicine, tissue engineering, and drug discovery.

Acknowledgements This study was supported in part by JSPS KAKENHI (Grant Nos. JP20H04539, JP20H05236, JP22H04564, and JP23KJ2110) from the Japan Society for the Promotion of Science (JSPS) and the MEXT-Supported Program for Private University Research Branding Project.

Compliance with ethical standards

Conflict of interest The authors declare no competing interests.

References

1. Uto K, Tsui JH, DeForest CA, Kim DH. Dynamically tunable cell culture platforms for tissue engineering and mechanobiology. Prog Polym Sci. 2017;65:53–82.
2. Gattazzo F, Urciuolo A, Bonaldo P. Extracellular matrix: a dynamic microenvironment for stem cell niche. Biochim Biophys Acta Gen Subj 2014;1840:2506–19.
3. Murphy WL, McDevitt TC, Engler AJ. Materials as stem cell regulators. Nat Mater. 2014;13:547–57.
4. Trounson A. The production and directed differentiation of human embryonic stem cells. Endocr Rev. 2006;27:208–19.
5. Grayson WL, Zhao F, Izadpanah R, Bunnell B, Ma T. Effects of hypoxia on human mesenchymal stem cell expansion and plasticity in 3D constructs. J Cell Physiol. 2006;207:331–9.
6. McBeath R, Pirone DM, Nelson CM, Bhadriraju K, Chen CS. Cell shape, cytoskeletal tension, and RhoA regulate stem cell lineage commitment. Dev Cell. 2004;6:483–95.
7. Zajac AL, Discher DE. Cell differentiation through tissue elasticity-coupled, myosin-driven remodeling. Curr Opin Cell Biol. 2008;20:609–15.
8. Chaudhuri O, Gu L, Darnell M, Klumpers D, Bencherif SA, Weaver JC, et al. Substrate stress relaxation regulates cell spreading. Nat Commun. 2015;6:6365.
9. Pelham RJ Jr, Wang YL. Cell locomotion and focal adhesions are regulated by substrate flexibility. Proc Natl Acad Sci. 1997;94:13661–5.
10. Chen CS, Mrksich M, Huang S, Whitesides GM, Ingber DE. Geometric control of cell life and death. Science. 1997;276:1425–8.
11. Cantini M, Donnelly H, Dalby MJ, Salmeron-Sanchez M. The plot thickens: the emerging role of matrix viscosity in cell mechanotransduction. Adv Healthc Mater. 2020;9:e1901259.
12. Kim D-H, Wong PK, Park J, Levchenko A, Sun Y. Microengineered platforms for cell mechanobiology. Annu Rev Biomed Eng. 2009;11:203–33.
13. Rajendran AK, Sankar D, Amirthalingam S, Kim HD, Rangasamy J, Hwang NS. Trends in mechanobiology guided tissue engineering and tools to study cell-substrate interactions: a brief review. Biomater Res. 2023;27:1–24.
14. Engler AJ, Sen S, Sweeney HL, Discher DE. Matrix elasticity directs stem cell lineage specification. Cell. 2006;126:677–89.
15. Engler AJ, Carag-Krieger C, Johnson CP, Raab M, Tang HY, Speicher DW, et al. Embryonic cardiomyocytes beat best on a matrix with heart-like elasticity: scar-like rigidity inhibits beating. J Cell Sci. 2008;121:3794–802.
16. Thiele J, Ma Y, Bruekers SMC, Ma S, Huck WTS. Designer hydrogels for cell cultures: a materials selection guide. Adv Mater. 2014;26:125–48.
17. Yu L, Ding J. Injectable hydrogels as unique biomedical materials. Chem Soc Rev. 2008;37:1473–81.
18. Li Z, Zhou Y, Li T, Zhang J, Tian H. Stimuli-responsive hydrogels: fabrication and biomedical applications. VIEW. 2022;3:20200112.
19. Amirthalingam S, Rajendran AK, Moon YG, Hwang NS. Stimuli-responsive dynamic hydrogels: design, properties and tissue engineering applications. Mater Horiz. 2023;10:3325–50.
20. Chang S, Wang S, Liu Z, Wang X. Advances of stimulus-responsive hydrogels for bone defects repair in tissue engineering. Gels. 2022;8:389.
21. Chen G, Hoffman AS. Graft copolymers that exhibit temperature-induced phase transitions over a wide range of pH. Nature. 1995;373:49–52.
22. Yoshida R, Uchida K, Kaneko T, Sakai K, Kikuchi A, Sakurai Y, et al. Comb-type grafted hydrogels with rapid deswelling response to temperature changes. Nature. 1995;374:240–2.
23. Jeong B, Bae YH, Lee DS, Kim SW. Biodegradable block copolymers as injectable drug-delivery systems. Nature. 1997;388:860–2.
24. Shimizu T, Yamato M, Kikuchi A, Okano T. Cell sheet engineering for myocardial tissue reconstruction. Biomaterials. 2003;24:2309–2016.
25. Yoshida R, Takahashi T, Yamaguchi T, Ichijo H. Self-oscillating gel. J Am Chem Soc. 1996;118:5134–5.
26. Irie M. Stimuli-responsive Poly(N-isopropylacrylamide). Photo- and chemical-induced phase transitions. Adv Polym Sci. 1993;110:49–50.
27. Matsuda N, Shimizu T, Yamato M, Okano T. Tissue engineering based on cell sheet technology. Adv Mater. 2007;19:3089–99.
28. Zhou Y, Ye H, Chen Y, Zhu R, Yin L. Photoresponsive drug/gene delivery systems. Biomacromolecules. 2018;19:1840–57.
29. Safavi-Mirmahalleh SA, Golshan M, Gheitarani B, Hosseini MS, Kalajahi MS. A review on applications of coumarin and its derivatives in preparation of photo-responsive polymers. Eur Polym J. 2023;198:112430.
30. Yamada N, Okano T, Sakai H, Karikusa F, Sawasaki Y, Sakurai Y. Thermo-responsive polymeric surfaces; control of attachment and detachment of cultured cells. Makromol Chem Rapid Commun. 1990;11:571–6.
31. Okano T, Yamada N, Sakai H, Sakurai Y. A novel recovery system for cultured cells using plasma-treated polystyrene dishes grafted with poly(N-Isopropylacrylamide). J Biomed Mater Res. 1993;27:1243–51.
32. Takahashi H, Nakayama M, Itoga K, Yamato M, Okano T. Micropatterned thermoresponsive polymer brush surfaces for fabricating cell sheets with well-controlled orientational structures. Biomacromolecules. 2011;12:1414–8.
33. Okada S, Sato E. Thermo- and photoresponsive behaviors of dual-stimuli-responsive organogels consisting of homopolymers of coumarin-containing methacrylate. Polymers. 2021;13:329.
34. Nakayama Y, Matsuda T. Photocycloaddition-induced preparation of nanostructured, cyclic polymers using biscinnamated or biscoumarinated oligo(ethylene glycol)s. J Polym Sci Part A Polym Chem. 2005;43:3324–36.
35. Liu J, Lou X, Schotman MJ, Marín San Román PP, Sijbesma RP. Photo-crosslinked coumarin-containing bis-urea amphiphile hydrogels. Gels. 2022;8:615.
36. Inal S, Kolsch JD, Sellrie F, Schenk JA, Wischerhoff E, Laschewsky A, et al. A water soluble fluorescent polymer as a dual colour sensor for temperature and a specific protein. J Mater Chem B. 2013;1:6373–81.
37. Chanthaset N, Takahashi Y, Haramiishi Y, Akashi M, Ajiro H. Control of thermoresponsivity of biocompatible poly(trimethylene carbonate) with direct introduction of oligo(ethylene glycol) under various circumstances. J Polym Sci Part A Polym Chem. 2017;55:3466–74.

38. Zhao J, Er GTK, McCallum FJ, Wang S, Fu C, Kaitz JA, et al. Photo/thermal dual responses in aqueous-soluble copolymers containing 1-naphthyl methacrylate. Macromolecules. 2021;54: 4860–70.
39. Ruskowitz ER, DeForest CA. Photoresponsive biomaterials for targeted drug delivery and 4D cell culture. Nat Rev Mater. 2018; 3:17087.
40. Zhang K, Feng Q, Fang Z, Gu L, Bian L. Structurally dynamic hydrogels for biomedical applications: pursuing a fine balance between macroscopic stability and microscopic dynamics. Chem Rev. 2021;121:11149–93.
41. Tang S, Richardson BM, Anseth KS. Dynamic covalent hydrogels as biomaterials to mimic the viscoelasticity of soft tissues. Prog Mater Sci. 2020;120:100738.
42. Yang C, Tibbitt MW, Basta L, Anseth KS. Mechanical memory and dosing influence stem cell fate. Nat Mater. **2014**; 13:645–52.
43. Nelson BR, Kirkpatrick BE, Miksch CE, Davidson MD, Skillin NP, Hach GK, et al. Photoinduced dithiolane crosslinking for multiresponsive dynamic hydrogels. Adv Mater. 2023;e2211209.
44. Yavitt FM, Kirkpatrick BE, Blatchley MR, Speckl KF, Mohagheghian E, Moldovan R, et al. In situ modulation of intestinal organoid epithelial curvature through photoinduced viscoelasticity directs crypt morphogenesis. Sci Adv. 2023;9: eadd5668.
45. Kosaka T, Yamaguchi S, Izuta S, Yamahira S, Shibasaki Y, Tateno H, et al. Bioorthogonal photoreactive surfaces for single-cell analysis of intercellular communications. J Am Chem Soc. 2022;144:17980–8.
46. Miyata T, Asami N, Uragami T. A reversibly antigen-responsive hydrogel. Nature. 1999;399:766–9.
47. Miyata T, Jige M, Nakaminami T. Tumor marker-responsive behavior of gels prepared by biomolecular imprinting. Proc Natl Acad Sci USA. 2006;103:1190.
48. Norioka C, Okita K, Mukada M, Kawamura A, Miyata T. Biomolecularly stimuli-responsive tetra-poly (ethylene glycol) that undergoes sol–gel transition in response to a target biomolecule. Polym Chem. 2017;8:6378–85.
49. Okihara M, Okuma K, Kawamura A, Miyata T. Photoresponsive gelation of four-armed poly (ethylene glycol) with photodimerizable groups. Gels. 2022;8:183.
50. Noguchi T, Akioka N, Kojima Y, Kawamura A, Miyata T. Photoresponsive polymer films with directly micropatternable surface based on the change in free volume by photo-crosslinking. Adv Mater Interfaces. 2022;9:2101965.
51. Noguchi T, Higashino M, Kodama N, Kawamura A, Miyata T. Cell patterning on photocrosslinkable polymer films with micropatternable surfaces. Responsive Mater. **2023**;1:e20230007.
52. Chen Y, Geh JL. Copolymers derived from 7-acryloyloxy-4-methylcoumarin and acrylates: 2. Reversible photocrosslinking and photocleavage. Polymer. 1996;37:4481–6.
53. Trenor SR, Long TE, Love BJ. Photoreversible chain extension of poly(ethylene glycol). Macromol Chem Phys. 2004;205:715–23.
54. Nagata M, Yamamoto Y. Synthesis and characterization of photocrosslinked poly(ε-caprolactone)s showing shape-memory properties. J Polym Sci Part A Polym Chem. 2009;47:2422–33.
55. Lutz JF. Polymerization of oligo(ethylene glycol) (meth)acrylates: toward new generations of smart biocompatible materials. J Polym Sci Part A Polym Chem. 2008;46:3459–70.
56. Trenor SR, Shultz AR, Love BJ, Long TE. Coumarins in polymers: from light harvesting to photo-cross-linkable tissue scaffolds. Chem Rev. 2004;104:3059–78.
57. Lewis FD, Barancyk SV. Lewis acid catalysis of photochemical reactions. 8. Photodimerization and cross-cycloaddition of coumarin. J Am Chem Soc. **1989**;111:8653–61.
58. Yonezawa N, Yoshida T & Hasegawa M. Symmetric and asymmetric photocleavage of the cyclobutane rings in head-to-head coumarin dimers and their lactone-opened derivatives. J Chem Soc Perkin Trans. 1983:1083.
59. Tasaki K. Poly (oxyethylene)– water interactions: a molecular dynamics study. J Am Chem Soc. 1996;118:8459–69.
60. Maeda Y, Kubota T, Yamauchi H, Nakaji T, Kitano H. Hydration changes of poly(2-(2-methoxyethoxy)ethyl methacrylate) during thermosensitive phase separation in water. Langmuir. 2007;23: 11259–65.
61. Lutz JF, Weichenhan K, Akdemir Ö, Hoth A. About the phase transitions in aqueous solutions of thermoresponsive copolymers and hydrogels based on 2-(2-methoxyethoxy)ethyl methacrylate and oligo(ethylene glycol) methacrylate. Macromolecules. 2007;40:2503–8.
62. Lutz JF, Akdemir Ö, Hoth A. Point by point comparison of two thermosensitive polymers exhibiting a similar LCST: is the age of poly (NIPAM) over? J Am Chem Soc. 2006;128:13046–7.
63. Butcher DT, Alliston T, Weaver VMA. tense situation: forcing tumour progression. Nat Rev Cancer. 2009;9:108–22.
64. Solon J, Levental I, Sengupta K, Georges PC, Janmey PA. Fibroblast adaptation and stiffness matching to soft elastic substrates. Biophys J. 2007;93:4453–61.
65. Okano T, Yamada N, Okuhara M, Sakai H, Sakurai Y. Mechanism of cell detachment from temperature-modulated, hydrophilic-hydrophobic polymer surfaces. Biomaterials. 1995;16:297–303.